Chapter-2

2 Methodology and Instrumentation

2.1 Materials used for Synthesis and other Applications

BSA (lyophilized powder, >96%, MW=66,430 Da), lysozyme (chicken egg white, single-chain 14kDa with isoelectric point 11.35), melatonin, glycine, hydrochloric acid, sodium dihydrogen phosphate, disodium hydrogen phosphate, rutile nanosized TiO_2, sodium chloride, hydrochloric acid, L-lysine, chloroauric acid ($HAuCl_4$. $3H_2O$) uric acid (UA), ascorbic acid (AA), and hypoxanthine (HX) were purchased from Sigma-Aldrich Chemical Co (USA). Phosphate buffers of different pH were prepared using sodium dihydrogen phosphate, disodium hydrogen phosphate, and phosphoric acid following the reported protocols. Synthetic melatonin tablets were purchased over the counter from a commercial medical shop in Varanasi, India. Double distilled (DD) water was used to prepare the aqueous solutions required for all the experiments. All reagents were of analytical grades and used directly without further purification.

2.2 Methodologies related to Self-assembled Phases of Bovine Serum Albumin to Synthesize Novel Functional Hydrogel for Skin Protection against UVB

2.2.1 Synthesis of Temperature-dependent Phases of BSA

All the temperature-dependent phases of BSA were synthesized using the single pot hydrothermal method. The homogenous solutions of concentration 40 mg/ml of lyophilized BSA powder were prepared using Sorensen's phosphate buffer (pH-7.4) with a sodium salt

concentration of 150 mM. The prepared solutions were transferred to a 25 ml Teflon cylinder with a steel autoclave and heated for the hydrothermal reaction at temperatures ranging from 25 ^{0}C to 120 ^{0}C for 15 h. During heating at different temperatures, different phases of BSA have resulted. The resultant samples were named according to their heating temperature. For example, H-100 suggests that the BSA solution has been heated at 100 ^{0}C for 15 h using the hydrothermal method. The schematic of the synthesis process with intermediate units and final phases is shown in Figure 2.1.

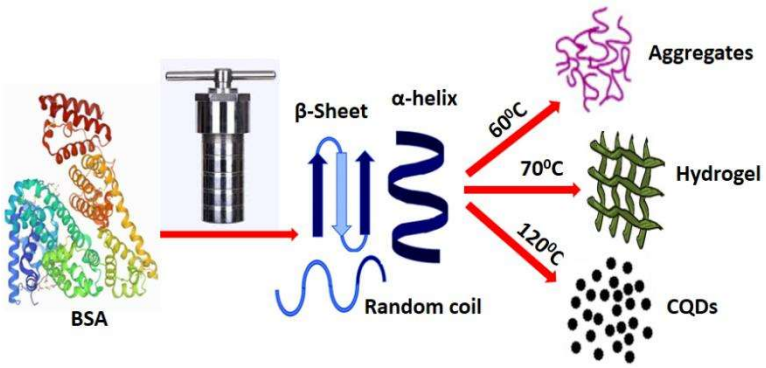

Figure 2.1 Synthesis process for temperature-dependent phases of BSA hydrogel

2.2.2 Cell Culture

For primary skin cell culture, skin tissue was collected from hairless skin of Swiss albino mice, and isolation of primary epidermal cells, endothelial cells, dermal cells, and fibroblast cells was performed following the protocol given by Pauline Henrot *et al.* (2020)[116]. For experimental purposes, epidermal cells were used.

2.2.3 Cell Viability

The biocompatibilities of all samples, i.e., H-25, H-60, H-70, H-80, H-90, H-100, H-110, H-120, and H-200 were determined by the MTT assay [3-(4,5-dimethylthiazol-2-yl)-2,5-

diphenyl tetrazolium bromide] where the primary mice skin cells were plated at 10^4 cells/well in 96-well plates (Genetix) 24h before experimentations. After completion of 24 h, cells were treated with H-25, H-60, H-70, H-80, H-90, H-100, H-110, H-120 and H-200 with same dose (20mg/ml, i.e., 1:1 sample: complete media). Complete media was added in control (with cells) and negative control or blank (without cells) groups. After 24 h of treatment, cells were processed for MTT assay following the laboratory standard process[117], and the optical density was measured in triplicate at 595 nm in a microplate reader (Biorad).

2.2.4 Cellular Uptake

For the cellular uptake study of each sample, primary mice skin cells were seeded at 6000 cells/well upon the round coverslips placed inside the 24 well plates 24 h before treatments. After 24 h, cells were treated with the samples (H-25, H-60, H-70, H-80, H-90, H-100, H-110, H-120, and H-200) at the 20 mg/ml concentration for the next 24 h, similarly to MTT assay. After 24 h, treated cells were fixed, permeabilized, and stained with DAPI according to the laboratory standard procedure33. Finally, images were captured by Carl Zeiss 780 LSM laser scanning confocal microscope (Germany).

2.2.5 UVB Treatment study

UVB lamp (G25T8E, Sankyo Denki) with peak emission at 306 nm was used to generate UVB radiation. The experiments were divided into two primary groups for the UVB treatment study, i.e., UVB treated and UVB+H-110 treated. Each group was further subdivided into three subgroups according to UVB exposures, i.e., 5 min, 10 min, and 15 mins according to [118]. For each subgroup, primary mice skin cells were seeded at 6000 cells/well on coverslip (3 wells) and 12000 cells/well in other three wells of 6 well plates [thus 3 separate 6 well plates for 5', 10' and 15' UVB treatment) for 24 h for acclimatization. After 24 h, every six well-plates were placed under UVB light of the self-

made UVB chamber shown in Figure 2.2 for respective 5', 10' and 15' UVB treatment. On the same day, cells of the UVB+H-110 group were first layered and incubated with H-110 for 1 h inside the CO_2 incubator. After 1 h, cells were treated with UVB as described above. After all treatments, cells seeded on the coverslips were fixed, permeabilized, and stained with DAPI. Images were captured by Carl Zeiss 780 LSM laser scanning confocal microscope (Germany) for cytological study. Other treated cells were processed for survival analysis through MTT assay.

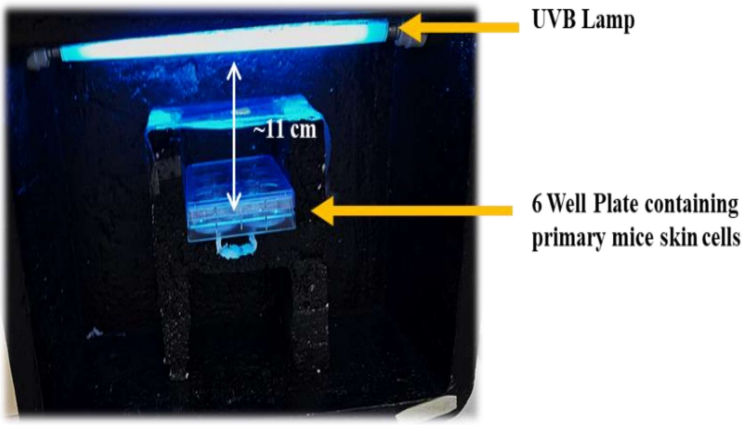

Figure 2.2 Setup for UVB radiation treatment chamber

2.2.6 *In vivo* Mice Model Study

Two weeks before experimentations, all-female Swiss albino mice (N=30) were maintained at 12 h light: 12 h dark cycle with 25 ± 2 ^{0}C temperature at the department of zoology, Banaras Hindu University, Varanasi, Uttar Pradesh, India. All maintenance procedures and experimentations were performed following the revised Animals Act Government of India, 2007 approved rules [Committee for the Purpose of Control and Supervision of Experiments on Animals (CPCSEA), Registration No.-1802/GO/Re/S/15/ CPCSEA].

After acclimatization, animals were divided into six following groups (a bunch of five animals) as listed below

1) Control (n = 5) - without any treatment

2) H-110 treated group (n = 5) - where a single layer of H-110 at the backside was applied to each animal,

3) 3 days UVB treated group (UV 3D, n = 5), treated with UVB for 20 min for 3 days,

4) 5 days UVB treated group (UV 5D, n = 5), treated with UVB for 20 min for 5 days,

5) 3 days H-110+UVB treated group (H-110+UV 3D, n = 5), where a single layer of H-110 at the backside was first applied and then UVB treatment was given for 20 min for 3 days,

6.) 5 days H-110+UVB treated group (H-110+UV 5D, n = 5), where a single layer of H-110 at the backside was first applied and then UVB treatment was given for 20 min for 5 days. During treatment, mild ether anesthesia was continually given to the animals. After completing the experimental periods, part of the treated skin was collected from each animal for further histoarchitectural analysis. No animals were sacrificed during this experimentation, as after skin collection, animals were given proper medical care to heal the wounds.

2.2.7 Morphometric Analysis

For histological analysis, skins were immediately removed from each group of animals and fixed in 10% formalin, followed by dehydration, clearing with xylene, and finally processed in wax and sectioned (7 microns) for hematoxylin and eosin staining (HE staining)[119]. Histoarchitectures were observed in randomly selected sections under a research microscope (Nikon E 200, Japan).

2.3 Methodologies Related to Synthesis of PNDs, Electrode fabrication, and Real Sample Analysis

2.3.1 Synthesis of BSA Derived Protein Nano Dots (PNDs)

A simple one-pot thermal aggregation via hydrothermal method has been employed to synthesize PNDs. Homogenous solutions of BSA (40 mg/ml, 300 mM NaCl salt concentration) were prepared using pH-7 Sorensen's phosphate buffer. The resulting solution was transferred to a teflon-lined steel autoclave and heated at 200 °C for 15h. The synthesized PNDs solution was centrifuged at 10k rpm for 10 min to remove debris and filtered through the syringe filters (Axiva, 0.2µm cut-off) to narrow down to particle size distribution. Finally, the PNDs solution was obtained and stored at room temperature for further characterization and sensing application.

2.3.2 Fabrication of Modified Sensors Electrode

Before modification, the glassy carbon electrode (GCE) was polished using alumina powder slurry (1µm, 0.3µm, and 0.05µm) on a micro cloth pad. After polishing, the electrode was rinsed thoroughly with double distilled water. 5µl of 40mg/ml stock solution of PNDs was then drop-casted on the polished GCE surface and dried for 1hr at 70°C in the hot air oven, and this modification was labeled as PNDs /GCE. Modified GCE was rinsed with distilled water and stabilized by recording voltammograms in phosphate buffer of pH-7 between -1.0 to +1.0V at $100mVs^{-1}$ till the overlapping voltammograms were not obtained.

For the conjugation of drop-casted PNDs with AuNP-poly Lysine, an aliquot of 1mM L-Lysine and 1mM chloroauric acid solution were taken in 1:1 (200µl:200µl) volume ratio. 2mL of pH-7 Phosphate buffer was added to the solution as the supporting electrolyte. The

in-situ electrochemical tailoring of PNDs was carried out by scanning 15 cyclic voltammograms in the prepared solution within a potential range of -1.0 to +1.8V scanned at a rate of 100mV/s. This modification was named Au-PLL/ PNDs /GCE. The surface-modified electrode was then rinsed with distilled water and further stabilized in the buffer solution.

2.3.3 Analytical Techniques and Sample Preparation

A stock solution of melatonin (1mM) was prepared by dissolving the required weight of solid melatonin (Mel) in double-distilled water. Any light-induced degradation of Mel was avoided by storing the stock solution in the dark. The required amount of stock solution was added to the electrochemical cell containing 2ml of PB-7 and the DD water to make the total solution of 4 mL. Both cyclic voltammetry (CV) and square wave voltammetry (SWV) was utilized to investigate the electrochemical behavior of melatonin. The SW voltammograms were recorded in the potential range of 0.4 - 1.0V, with the potential step of 6mV. The optimized amplitude and frequency were found to be 25mV and 10.0Hz, respectively. The same potential range was used for recording cyclic voltammograms. The sensing surface was rinsed in DD water and stabilized in a buffer solution in the potential range of 0.2 - 1.0V after every SWV scan.

2.3.4 Pharmaceutical Tablet Analysis

The local medical store-purchased tablets (Altonil, Alteus Biogenics Pvt Ltd.) containing Mel (3 mg/tablet). Each tablet was weighed and turned into a fine powder using a mortar and pestle. A fixed amount of tablet powder was then dissolved in distilled water to obtain the 1mM Mel concentration. The solution was passed through 125mm Whatman filter paper to remove the undissolved particles. The stock solution was then used to prepare the required concentrations.

2.3.5 Biological Sample

To investigate the performance of modified electrodes in real samples, urine and mung bean seed paste were taken as test samples. A urine sample was collected from a healthy volunteer (Female, age 30) just before sleeping at night. The urine sample was centrifuged and diluted four times with pH-7 phosphate buffer to remove complexities. For recovery studies, a diluted urine sample was spiked by the required amount of 500µM Mel stock solution.To prepare a test sample from mung beans, 10 uniform-sized seeds were soaked in DI water for 12 h and later converted into a paste using mortar-pestle. This paste was diluted with 2ml pH-7 phosphate buffer and directly used for recovery studies by spiking the required amount of 500µM Mel stock solution.

2.4 Methodologies Related to Synthesis of PNDs, MPNDs for Drug Delivery Carrier with Enhanced Biological Efficacy of Melatonin

2.4.1 Synthesis of PNDs and MPNDs

The synthesis of the PNDs was carried out via a hydrothermal method.[120,121] The homogenous solutions of lysozyme (40 mg/mL) were prepared at two different pH (pH-2 and pH-7 buffer) using a glycine-HCl buffer and Sorensen's phosphate buffer respectively). For hydrothermal reaction, the prepared solutions were transferred to a 200ml Teflon cylinder with a steel autoclave and heated at 200oC for 15 h. Further, solutions were cooled down and centrifuged at 10k rpm for 10 min. The supernatant was collected and filtered using the syringe filters (Axiva, 0.2µm cutoff) to get the homogenous particle size.

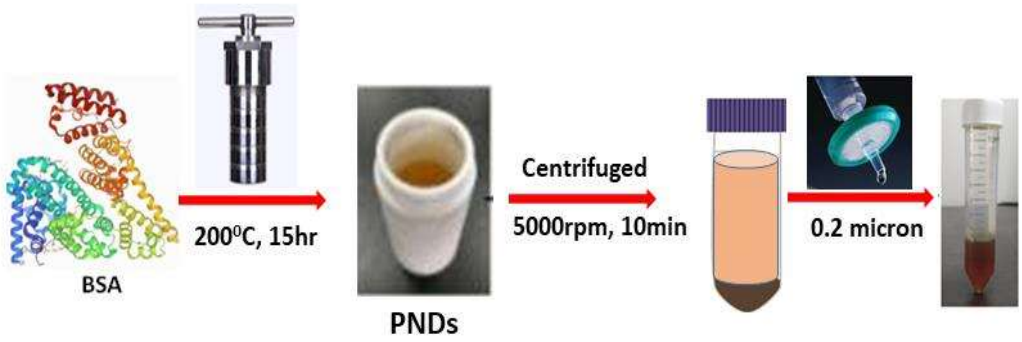

Figure 2.3 Schematic of synthesis procedure of PNDs using hydrothermal method

2.4.2 Fluoresce Quantum Yield Calculation

The relative quantum yield of PNDs was evaluated with respect to quinine sulfate (Sigma Aldrich India Ltd.). A standard curve was plotted between integrated fluorescence intensity values with respect to absorbance (<0.1) for different quinine sulfate (QS) solution concentrations, prepared in 0.1 M H_2SO_4. A similar procedure was also followed for the PNDs suspension, with deionized water acting as diluents. The slope, obtained from the linear fit standard curves, was used to calculate the quantum yield using equation 1.

$$\Phi x = \Phi st \times \frac{Gradx}{Gradst} \times \frac{\eta 2x}{\eta 2st} \dots\dots\dots\dots\dots\dots (1)$$

Φ_x= Quantum yield of CQDs, Φ_{st}=Quantum yield of standard, $Grad_x$= Gradient of curve plotted for CQDs, $Grad_{st}$= Gradient of curve plotted for standard, η_x= Refractive index of solvent used for preparing CQDs solution, η_{st}= Refractive index of solvent used for preparing QS standard. The quantum yield of QS has been estimated to be 0.54 in H_2SO_4 solution. The refractive index for 0.1M H_2SO_4 was taken to be the same as DI water.

2.4.3 Cell Culture

The human MG63 and MDA-MB-231 cancer cell lines were procured from the National Centre for Cell Science (NCCS) Pune and cultured in Dulbecco's Modified Eagle Medium (DMEM) (High Glucose) with 10% FBS, 0.1 mM Minimum Essential Medium (MEM) Non-Essential Amino Acid (NEAA), 1% penicillin-streptomycin and 2 mM L-glutamine, as supplements. Cells were grown in T25 flasks with vented caps (Genetix) in a humidified atmosphere (Thermo scientific, Heracelvios 160i) at 37°C with 5% CO_2. No contamination was observed in the cell line used for the experiments.

2.4.4 Cell Viability Assay

The cytotoxicity of the PNDs was determined by the 3-(4, 5-dimethylthiazol-2-yl)-2,5-diphenyl tetrazolium bromide (MTT) assay in MG63 cells. MG63 cells were cultured in flat bottomed 96-well plates (Genetix) at 10^4 cells/well for 24 h before the treatment. Cells were treated with complete media containing 10% FBS. To find the physiological dose at which the PNDs further could be used for bioimaging and drug delivery, cells were plated into five groups (control and different dosages of PNDs, i.e., 2 mg/100µl, 4 mg/100µl, 10 mg/100µl, and 20 mg/100µl) for 24 h.

To determine the working dosage of Mel in breast cancer studies, we performed a dose-dependent study with six different concentrations (0.1-1 mM) of Mel in MDA-MB-231 cells[122]. After incubation, the MTT assay was performed according to standard protocol[123,124]. Cytotoxicity was measured by determining the change of color formed due to the formazan from 3-(4,5-dimethylthiazol-2-yl)-2,5-diphenyl tetrazolium bromide salt and the absorbance of the colored medium was measured at 595 nm using a microplate reader (Instrument). The percent viability was calculated by taking the viability of control cells as 100%. To evaluate the cytotoxic effect of Mel alone and MPNDs on cell

proliferation, an MTT assay was performed in MDA-MB-231 cells by treating with Mel and MPNDs along with no treated control group after incubation of 24 h, 48 h, and 72 h.

2.4.5 Cell Migration Assay

Cell migration capability was evaluated by wound closure assay. MDA-MB-231cells were seeded into 6 well plates for 24 h, and a vertical wound was made down through the cell monolayer by using a 200µl sterile micro tip by pressing firmly against the top of each well. The culture media containing cell debris from each well was removed gently without disturbing the cells and treated with the derived concentration. In the control group, only complete DMEM media was added. Images were taken at an interval of 2 h, starting from treatment time up (0 h) to 6 h. The quantitative analysis of the collective cell migration assay was performed by measuring the wound closure area using the following formula;

$$\text{Wound Closure } \% = [(A_{t=0h} - A_{t=\triangle h})/A_{t=0h}] \times 100\%$$

($A_{t=0h}$ is the area of the wound measured immediately after scratching (t=0h), and $A_{t=\triangle h}$ is the area of the wound measured h hours after the scratch is performed [125].

2.4.6 Cellular Uptake Studies

One day before treatment, MG63 and MDA-MB-231 cells were seeded at 6 x 10^3 cells per well on the cover slides, which are placed in the 24 well culture plate. MG63 cells were then treated with 20mg of pH-2 PNDs and pH-7 PNDs for 24 h at 37°C. Subsequently, MDA-MB-231 cells were treated with Mel and MPNDs for 24 h at 37°C. At 1:5000 concentration of DAPI nuclear stain was added to the cells after 24 h of treatment. Finally, images were captured by a Fluorescence microscope and confocal microscopy system.

2.4.7 Statistical analysis

All statistical analysis was performed with a one-way analysis of variance (ANOVA) test, and the results are represented as mean ± SEM.

2.5 Characterization Techniques and Instruments

2.5.1 UV –Vis Spectrophotometer

UV-Vis measurements were carried out using Eppendorf Biospectrometer and JASCO V770 UV-Vis spectrophotometer. UV-Vis spectrometry is a technique to measure the light absorbed by the material across the ultraviolet and visible range of the electromagnetic spectrum. Light can be absorbed, transmitted, or reflected when light falls on a matter. Absorbance in the UV-Vis region can cause atomic excitation, which initiates the molecule's transition from a lower energy state to an excited state. To change the excitation state, molecules must absorb a sufficient level of radiation for an electron to move lower to a higher molecular orbit which shows accordance with the fact that short bandgap material is correlated to the absorbance of the shorter wavelength of light, which makes materials to electrochemically specific and can be used to quantify the analytes in a sample based on their absorption characteristic[126].

A UV-Vis spectrophotometer measures the intensity of light transmitted through a sample compared to a reference measurement of the incident light source. The Eppendorf Biospectrometer uses a pulsed Xenon flash lamp to interrogate micro-volume samples with light across a 200-800nm wavelength. A CMOS photodiode array acquires the transmitted light with a wavelength accuracy of 0.5nm. The concentration of unknown liquid samples can be calculated by Beer-Lambert Law. According to this law, the amount of light

absorbed is directly proportional to the concentration of the sample and the distance the light travels through the sample, the path length.

$$A = \log 10 \left(\frac{\mathrm{Io}}{\mathrm{I}}\right) = \varepsilon \mathrm{CL}$$

Where A is the measured absorbance, I_0 is the intensity of the incident light at a given wavelength, I is the transmitted intensity, L is the path length of the cuvette, C is the concentration of the absorbing material, and ε is a constant known as the molar absorptivity or extinction coefficient.

JASCO V770 UV-Vis/NIR spectrophotometer was used to measure solid materials' absorbance at 190-2700nm. A sample is placed in front of the integrating sphere. Light from an optical source is transmitted through the sample and enters the integrating sphere. The light is then reflected by the internal surface of the sphere and reaches the detector. Both the overall transmittance and the direct transmittance can be measured. The absorbance percentage is the percentage of the incident beam absorbed by the sample, i.e., that part of the beam that is neither reflected nor transmitted. Absorbance can be calculated from the reflectance and transmittance:

$$\%A = 100\% - \%R_{overall} - \%T_{overall}$$

2.5.2 Photoluminescence Spectrophotometer

Photoluminescence (PL) properties of synthesized carbon quantum dots and hydrogels have been carried out using HORIBA Fluorolog-QM. The HORIBA Fluorolog-QM series of modular research grade spectro-fluorometers is the fourth generation of the HORIBA Fluorolog.

Photoluminescence is a reliable and non-destructive technique used to characterize the optoelectronic properties of materials. Photoluminescence is a spectrochemical method where irradiation of the analyte at a specific wavelength leads to the emission of radiation at a different wavelength. When molecules absorb the incident excitation wavelength, the electronic state of the molecules changes from the ground state to one of the electronically excited states. During the relaxation from these excited states, they undergo one of the radiative and non-radiative decay processes. Fluorescence is one of the radiative decay processes with a short lifetime (picosecond to 100 nanoseconds) compared to other processes like collision deactivation, intersystem crossing, and phosphorescence. Analyzing the spectrum of the emitted light makes it possible to measure the response of the materials in terms of intensity as a function of wavelength. This gives access to information about the fluorescence intensity, band structure, relative light generation efficiency, and material quality. The photo-spectrometer contains four major components: a light source, an adjustable monochromator, a sample holder, and a detector, as shown in Figure 2.4. Steady-state fluorescence measurements require a continuous excitation source. This is usually a continuous xenon lamp that generates intense white light from 230 nm to the near-infrared range. The monochromators are diffraction grating or prism, which selects the excitation and emission wavelengths and monitors and corrects fluctuations in source light intensity. Double monochromators provide better stray light rejection and a higher signal-to-noise ratio for the instrument. The emission light, which is of a longer wavelength than the excitation, is filtered by the emission monochromator. This selects the wavelength of the light that reaches the detector, typically a photon-counting photomultiplier tube (PMT). PMT detectors are capable of detecting single photons, so the monochromator must effectively reject any unwanted light to avoid any background on the emission spectrum.

The excitation and emission paths are set at an angle of 90∘ to each other to minimize the fraction of excitation light entering the emission arm.

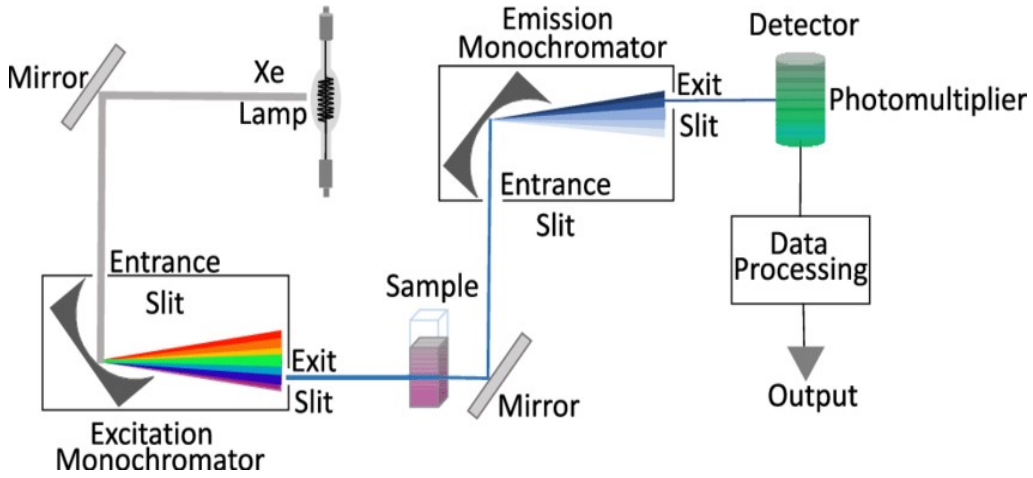

Figure 2.4 Ray diagram to explain the mechanism of the spectrophotometer[127]

2.5.3 Fourier Ransform Infrared Spectrophotometer

Fourier Transform Infra-Red (FTIR) spectroscopy was performed over the wavenumber 500-4000 cm^{-1} region with the resolution of 4 cm^{-1} using the Thermo Scientific Nicolet iD7 spectrometer. Samples under test were mixed with KBr, pelletized, and used for measurement at room temperature.

FTIR is concerned with the vibration of molecules. The basic premise of any infrared or vibrational spectroscopy technique is the observation of how light is scattered or absorbed upon reaching a material. In inelastic collisions between infrared light and molecules (either at the surface of a solid material or as a gas or liquid), some collisions produce characteristic vibrations of varying modes dependent on the nature of the bond itself but with a characteristic vibrational frequency. Vibrational energy is related to the molecule's reduced mass and spring constant. Since each functional group is composed of different atoms and

bond strength, the interaction of IR with these materials corresponds to a unique class of active groups present on the surface. The collection of energy bands represents a molecular fingerprint of the sample.

The three major parts of an FTIR are the source, interferometer, and detector. The source is typically a broadband emitter such as a mid-IR ceramic source (50-7,800 cm^{-1}), a near-IR halogen lamp (2,200 – 25,000 cm^{-1}), or a far-IR mercury lamp (10-700 cm^{-1}). The interferometer consists of a beamsplitter with a stationary mirror, a moving mirror, and a timing laser. The beamsplitter splits the light from a source into two perpendicular paths, with half the light going to a stationary mirror and the other half going to a moving mirror, as shown in Figure 2.5.

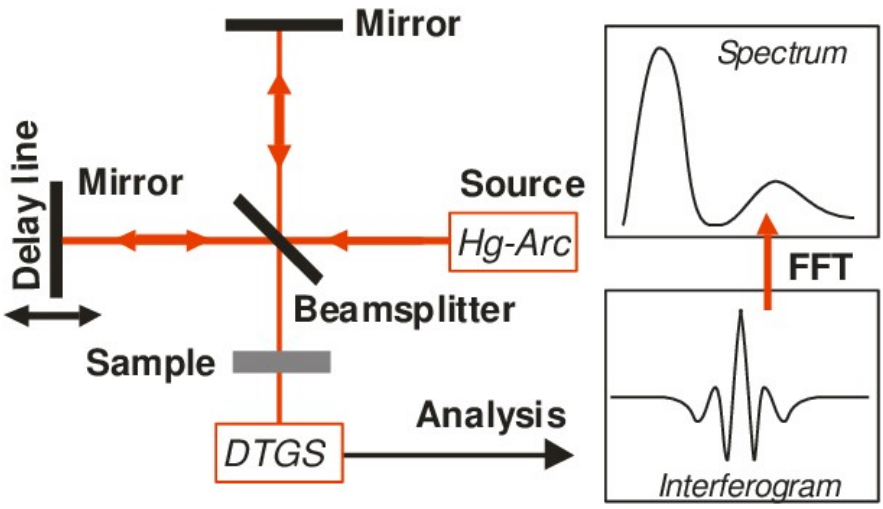

Figure 2.5 Ray diagram to explain the mechanism of Fourier transform infrared spectroscopy[128]

Common beamsplitter materials are KBr (375 – 12,000 cm^{-1}) for mid-IR, quartz (4,000 – 25,000 cm^{-1}) for near-IR, and mylar (30 – 680 cm^{-1}) for far-IR. The beams from the moving and stationary mirrors are recombined back at the beamsplitter and steered toward the

sample. The difference in the path of the mirrors causes constructive and destructive interference over the course of time it takes for the moving mirror to make a pass. The signal versus mirror position (and, thus, time) is called an interferogram. A laser is used to determine the position of the moving mirror using the precisely known wavelength of the laser. HeNe lasers are the industry norm due to their excellent wavelength stability compared to solid-state or diode lasers. The light is then steered through the sample and onto a detector. Detectors convert photons into measurable electric signals to be sent to the computer, where the time domain signal is converted to the frequency domain via a Fast Fourier Transform. Common detectors include room temperature DLaTGS for routine analysis, liquid nitrogen cooled MCT for high sensitivity applications, Si-photodiodes for visible and near-IR, and silicon bolometers for the far-IR.

2.5.4 Zetasizer Pro

The Zetasizer Pro is an instrument to measure a wide range of sample types and concentrations. It offers broad dynamic concentration capability and high sensitivity due to the Non-Invasive Back Scatter (NIBS) optical design. Measurements of particle size, electrophoretic mobility, zeta potential, and molecular weight can be easily performed. In this thesis, the Zeta potential of solutions was measured by Malvern Panalytical Zetasizer Pro. In practice, the zeta potential of dispersion is measured by applying an electric field across the solution. Figure 2.6 shows the mechanism of measurement of the zeta potential ray diagram. Particles within the dispersive medium with a zeta potential will migrate toward the electrode of opposite charge with a velocity proportional to the magnitude of the zeta potential. Due to the electric field, particles will move at different speeds: highly charged particles will move faster than less charged particles. This velocity is measured using the technique of the laser Doppler anemometer. The frequency or phase

shift of an incident laser beam caused by these moving particles is measured as particle mobility. This mobility is converted to the zeta potential by inputting the dispersant viscosity and dielectric permittivity and the application of the Smoluchowski theories.

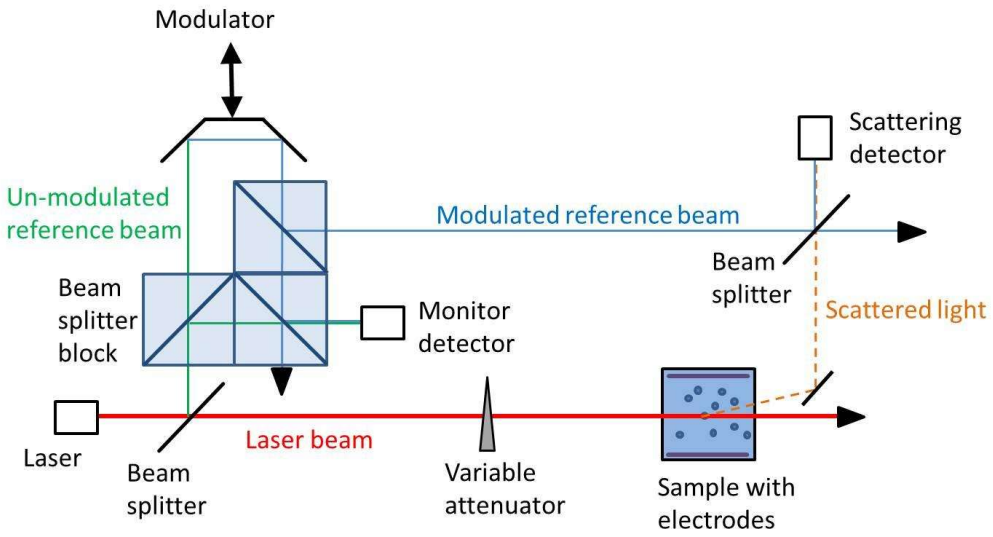

Figure 2.6 Ray diagram to explain the mechanism of Zeta Potential measurement[129]

2.5.5 X-ray Photoelectron Spectrophotometer

X-ray Photoelectron Spectroscopy spectrums were recorded using K-α, Thermo Fisher Scientific equipped with a monochromatic Al-Kα micro-focused X-ray source (100-4000 eV). The energy resolution was set at 0.1 eV at pass energy 1486.4 eV.

X-ray photoelectron spectroscopy (XPS), also known as electron spectroscopy for chemical analysis (ESCA), analyzes a material's surface chemistry. XPS can measure the elemental composition and the chemical and electronic state of the atoms within a material. This technique uses an x-ray beam to excite the molecules on the surface of a sample, leading to a release of photoelectrons. By analyzing the energy of these photoelectrons, we can learn crucial elemental and chemical binding information about a material's surface. XPS

measurements are conducted under ultra-high vacuum (< 10^{-8} Torr) to avoid collision between photoelectrons and gas molecules in the spectrometer and minimize surface contamination from residual gases. Figure 2.7 shows the schematic diagram of an XPS measurement system consisting of an X-ray source, an electron energy analyzer, and a photoelectron detector. Al-Kα (1486.6 eV) and Mg-Kα (1253.6 eV) are most commonly X-ray sources. By using monochromatized X-rays with a narrow linewidth, satellite spectra exited by $K\alpha_{3,4}$ and Kβ lines can be eliminated, and the energy resolution of photoelectrons improved. The ejected photoelectrons are transferred to an electron energy analyzer through the electron lens and separated according to their kinetic energy. The electron lens system between the sample and analyzer retards the photoelectrons, enhancing the energy resolution of the analyzer (0.1 eV). Various analyzers are used for these purposes, including the electrostatic hemispherical analyzer (HSA), the cylindrical mirror analyzer, and the spherical mirror analyzer. Among these, HSA is the most commonly employed. Following energy analysis, the photoelectrons are detected by such devices as electron multipliers or channel plates.

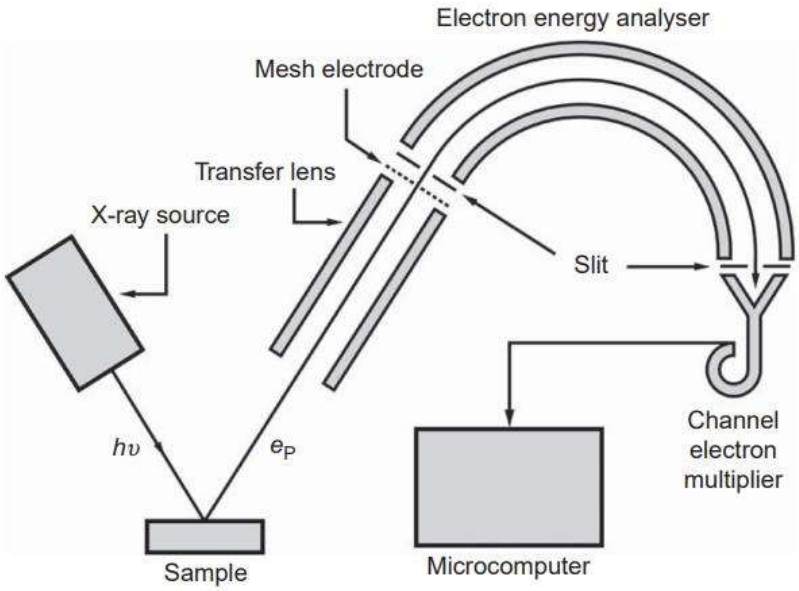

Figure 2.7 Schematic diagram of an XPS measurement system equipped with an electrostatic hemispherical analyser[130]

2.5.6 Small-angle X-ray Scattering (SAXS) Instrument

Xenocs SAS, model Xeuses 2.0 with dual-source module X-ray source (Q range varies from 0.005 to 1.2 Angstrom^{-1}) was used for small-angle X-ray Scattering (SAXS) measurement.

SAXS is a powerful method to gather quantitative nanoscale information from various samples, from liquids to pastes, powders, and films. The typical probing scales range is from ~1-100 nm, corresponding to the typical feature sizes of nanoparticles, block copolymers, and proteins. This versatility enables the characterizations of diverse samples, including nanoparticle solutions, nanocomposites, block copolymers, mesoporous materials, and protein solutions. Most SAXS experiments are carried out in transmission mode with the incident X-ray beam pointed directly at the sample. The scattered beam is then detected using a 2D area detector on the other side, as shown in Figure 2.8. The beam is sensitive to spatial variations in electron density. It can scatter from any interface that

changes electron density, such as polymer-polymer, polymer-solvent, protein-solvent, or solid-pore interfaces. The higher the contrast in electron density, the greater the intensity of the scattered beam. Beyond the frequency of these interfaces, the scattering profile also corresponds to the spatial arrangement of the interfaces and thus gives significant morphological details. For example, the conformation of proteins in solution and the size and shape of nanoparticles may be determined quantitatively. The results from a SAXS experiment correspond to the complete measured ensemble, typically about 0.1-1 mm3 which corresponds to ~1018 measured samples of a 100 nm motif.

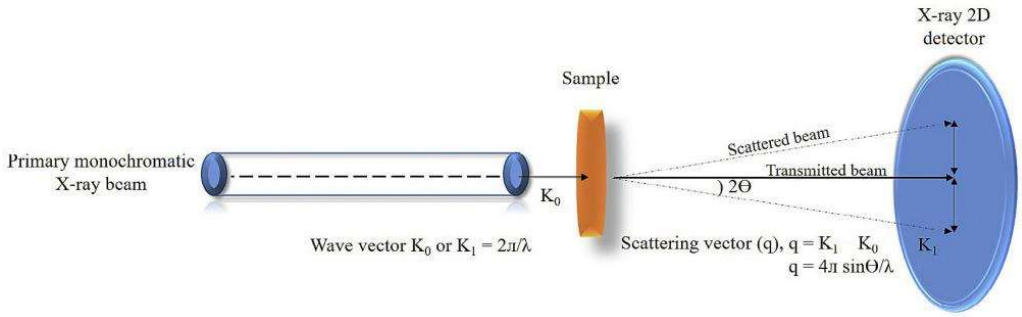

Figure 2.8 Schematic of SAXS measurement system[131]

2.5.7 Transmission Electron Microscope

Particle size and morphology of PNDs were studied by Transmission Electron Microscopy (TECNAI-T-20 -FEI instrument) at 200 kV accelerating voltage.

Transmission electron microscopy (TEM) is a microscopic technique in which a beam of electrons is transmitted through a specimen to form an image. TEM is capable do imaging at a significantly higher resolution than light microscopes, owing to the smaller de Broglie wavelength of electrons. This enables the instrument to capture fine detail—even

as small as a single column of atoms, which is thousands of times smaller than a resolvable object seen in a light microscope.

$$\lambda_e = \frac{h}{\sqrt{2m_0E\left(1+\frac{E}{2m_0c^2}\right)}}$$

TEM consists of an emission source or cathode, which may be a tungsten filament, needle, or lanthanum hexaboride (LaB_6) single crystal source. The gun is connected to a high voltage source (typically ~100–300 kV). Given sufficient current, the gun will begin to emit electrons either by thermionic or field electron emission into the vacuum. After it leaves the gun, the beam is typically accelerated by a series of electrostatic plates until it reaches its final voltage and enters the next part of the microscope: The condenser lens system. Typically a TEM consists of three stages of lensing. The stages are the condenser lenses, the objective lenses, and the projector lenses. The condenser lenses are responsible for primary beam formation.

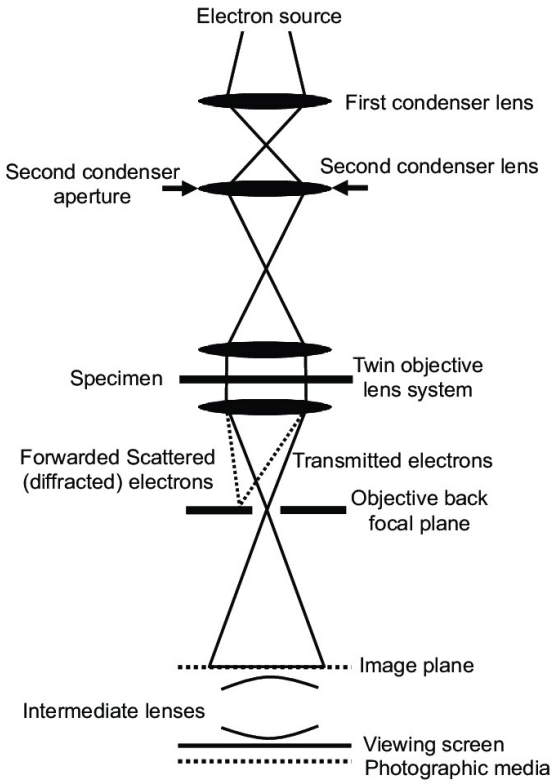

Figure 2.9 Schematic of the working process of TEM[132]

In contrast, the objective lenses focus on the beam that comes through the sample (in STEM scanning mode, there are also objective lenses above the sample to make the incident electron beam convergent). The projector lenses are used to expand the beam onto the phosphor screen or other imaging devices, such as film. The magnification of the TEM is due to the ratio of the distances between the specimen and the objective lens' image plane. The working process of TEM is shown in Figure 2.9. Imaging systems in a TEM consist of a phosphor screen, which may be made of fine (10–100 μm) particulate zinc sulfide, for direct observation by the operator, and, optionally, an image recording system such as photographic film, doped YAG screen coupled CCDs, or another digital detector. Typically these devices can be removed or inserted into the beam path by the operator as required.

2.5.8 Scanning Electron Microscope

Field Emission Scanning Electron Microscope (FESEM) images were collected using FEI Nova NanoSEM 450 FESEM. The working mechanism of SEM is similar to TEM. The main difference between SEM and TEM is that TEM uses transmitted electrons (electrons passing through the sample) to create an image. Instead, SEM creates an image by detecting reflected or knocked-off electrons, as shown in Figure 2.10. As a result, TEM offers valuable information on the inner structure of the sample, such as crystal structure, morphology, and stress state information. At the same time, SEM provides information on the sample's surface and its composition. SEMs use a specific set of coils to scan the beam in a raster-like pattern and collect the scattered electrons.

In SEMs, samples are positioned at the bottom of the electron column, and electron detectors capture the scattered electrons (back-scattered or secondary), as shown in Figure 2.10. Photomultipliers are then used to convert this signal into a voltage signal, amplified to create the image on a PC screen. Moreover, one of the most pronounced differences between the two methods is the optimal spatial resolution that they can achieve. SEM resolution is limited to ~0.5 nm, while with the recent development in aberration-corrected TEMs, images with a spatial resolution of even less than 50 pm have been reported.

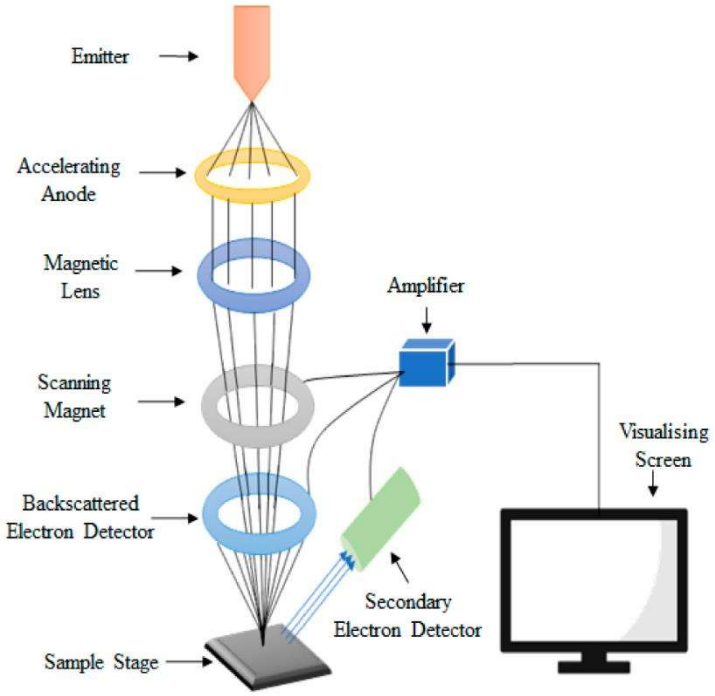

Figure 2.10 Schematic diagram of the working process of SEM[133]

2.5.9 Energy Dispersive X-ray (EDX) Spectrophotometer

The Energy Dispersive X-ray (EDX) microanalysis is an elemental analysis technique associated with scanning or tunneling electron microscopy. The generation of characteristic X-rays from the specimens reveals the material's elemental composition. The EDX microanalysis is used to confirm the complex phase formation, completeness of the reaction, and chemical composition of the outer and inner surfaces of composites. The spectrum of EDX microanalysis contains both semi-quantitative and information. EDX technique helps study the purity of drugs, synthesized hybrid materials, and nanoparticle compositions, which increases the agents' therapeutic performance. EDX is also used to study environmental pollution and to characterize mineral bioaccumulated in the tissues. In conclusion, the EDX can be a valuable tool for verifying elemental composition for endogenous and exogenous studies for tissue, cells, and other materials[134].

2.5.10 Confocal Microscopy

Carl Zeiss 780 LSM laser scanning confocal microscopy system (Germany) was used for fluorescence microscopy. A confocal microscope provides more focused and bright images than a fluorescence microscope. The primary function of a confocal microscope is to produce a point source of light that can penetrate deep tissues for optical sectioning for 3D reconstructions. The basic principle of a confocal microscope is based on the rejection of out-of-focus light, which is gained by the illumination and detection focused on the same diffraction-limited spot, making them confocal. By this method, anything outside the focal plane contributes little to the image and reduces the hazing used to observe in standard light microscopy with thick samples. Figure 2.11 shows a schematic of the core optics in a modern confocal microscope. The essential components of a modern confocal microscope are the point laser source with pinholes, the objective lenses, low-noise detectors with fast scanning mirrors, and filters for wavelength selection.

These point laser light sources are more stable, uniform, produce less heat, and emit a broad range of visible wavelengths. Zirconium arc light source was used to provide a point source of light which is focused on the sample by the first objective lens. The second objective lens focused the illuminated sample point onto the second pinhole in front of the detector. The illuminated sample stage could be moved in x and y directions to build the resulting image. Due to the light-rejecting nature of a confocal microscope, detectors are primarily highly sensitive photomultipliers (PMTs).

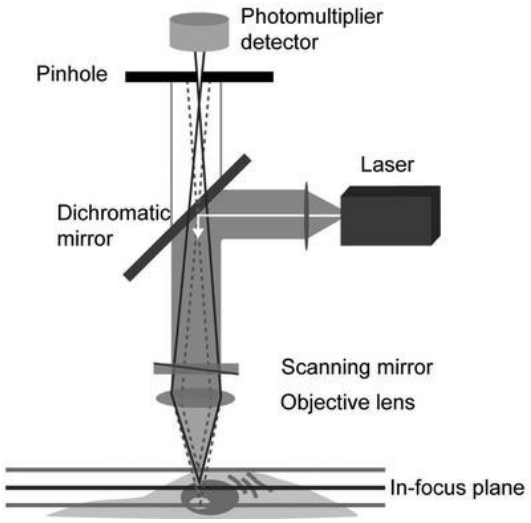

Figure 2.11 Components of a confocal microscope[135]

2.5.11 Rheometer

Rheological characterization of BSA hydrogels was performed using Anton Paar Physica MCR301 rheometer. Rheological geometry of 8 mm parallel plates having a gap of 1 mm at room temperature was used for rheological studies. The measurement for storage and loss modulus as a function of strain and frequency was also performed for all hydrogels between the frequency range of 0.1 and 10 rad s^{-1} with a constant strain of 0.5% at 25 ^{0}C. Figure 2.12 show the design of a combined motor and transducer rheometer. The physical properties of some fluids cannot be just defined by viscosity; they need more parameters to determine their physical states. Rheometers help measure the viscoelastic properties of these dense fluids by measuring the stress/ strain applied by the fluid in response to the applied force. There are two types of rheometers based on their working principle. The rotational or shear rheometer controls the shear stress or shear strain, whereas the rheometer that applies external stress or extensional strain is called the extensional rheometer. We have used a rotational rheometer for viscoelastic measurement of the hydrogels, which contains a sample holder, non-contact motor, and displacement sensor, which measure the

rotation or strain. Usually, the rheometer works in two modes. First is the native strain-controlled mode, where the user-defined shear strain is applied, and the instrument measures the resulting shear stress. The other mode is the native stress control mode, where user-defined shear stress is applied to the sample, and the instrument measures the resulting shear strain.

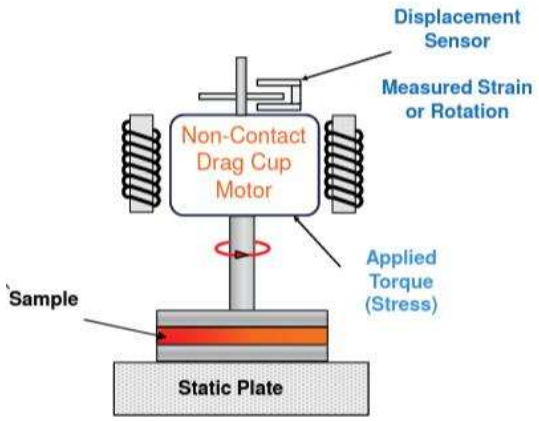

Figure 2.12 Design of single rotational head with combined motor and transducer rheometer[136]

Different geometries such as concentric cylinders, plate- plate, and cone- plate can be used for viscoelastic measurement according to their flow. In a parallel plate system, the material is confined between the gaps and does not flow out due to the capillary forces. The torque is calculated by one of the rotating plates and converted into other parameters.

2.5.12 Electrochemical voltammetry

PalmSens 3 voltammetric analyzer was used for electrochemical deposition and qualitative and quantitative studies. Three electrode systems in a glass cell with a phosphate buffer as a supporting electrolyte have been used for all the electrochemical experiments. The cell consists of Ag/AgCl (3M KCl), platinum wire, and glassy carbon as a reference, counter, and working electrode. Figure 2.13 shows the schematic diagram of the standard

electrochemical sensing setup. Any electrochemical sensing setup has three essential components: a glassy cell, potentiostat, and processor. In a glassy cell, a three-electrode system is submerged in an electrolyte medium, and most of the redox reaction occurs at the working electrode. The other component is a workstation or potentiostat. This digital device controls the glassy cell's reaction by injecting current into the cell through an Auxiliary, or Counter, electrode. The potentiostat measures the current flow between the Working and Counter electrodes in almost all applications. The 3rd one is the processor, which shows the results of the potentiostat in digital form.

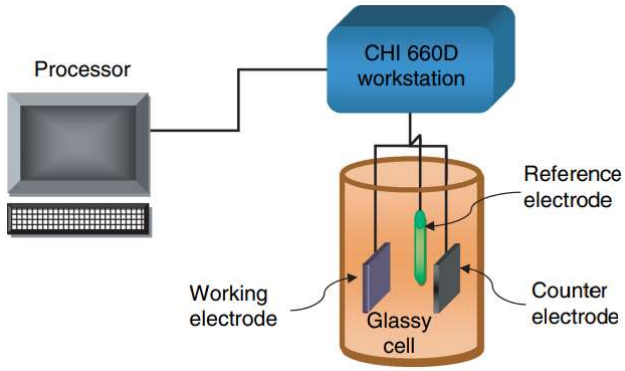

Figure 2.13 Schematic of electrochemical sensing setup[137]

There are three main types of electrochemical sensors: potentiometric, amperometric, and conductometric. Local equilibrium is established at the sensor interface for potentiometric sensors, where either the electrode or membrane potential is measured. Information about the composition of a sample is obtained from the potential difference between the two electrodes. Amperometric sensors exploit the use of a potential applied between a reference and a working electrode to cause the oxidation or reduction of an electroactive species; the resultant current is measured. On the other hand, conductometric sensors are involved in measuring conductivity at a series of frequencies.

In this thesis, electrochemical sensing has been done by cyclic voltammetry (CV) and square wave voltammetry (SWV). CV is the basic electrochemical test in which the current is recorded from positive to negative and negative to positive between the chosen window of potential. The information obtained from CV can be used to learn about the electrochemical behavior of the material. A typical cyclic voltammogram gives information about the redox peaks, which helps predict the electrode's capacitive behavior. Hence, the potential at which the material is oxidized and reduced can be found.

In comparison, SWV is one of the fastest and most sensitive pulse voltammetry techniques. This technique enables the evaluation of the kinetics and mechanism of the electrode process directly by the parameters involved in measurement. In SWV, the shape of the potential current curve is derived from the application of potentials of height pulse amplitude, which vary according to a potential step and period. The electric currents are measured at the end of the direct and reverse pulses. The signal is obtained as the intensity of the resulting differential current. This technique offers excellent sensitivity and high rejection to capacitive currents, which makes it one of the best techniques for sensing applications.